NMR Studies of the Antibody-Bound Conformation of a Carbohydrate-Mimetic Peptide[†,‡]

Margaret A. Johnson, Archimede Rotondo, and B. Mario Pinto*

Departments of Chemistry and of Molecular Biology and Biochemistry, Simon Fraser University, Burnaby, British Columbia, Canada V5A 1S6

Received October 12, 2001; Revised Manuscript Received December 3, 2001

ABSTRACT: Transferred nuclear Overhauser enhancement (TRNOE) experiments have been performed at 800 MHz to investigate the bound conformation of the hexapeptide DRPVPY, a functional molecular mimic of the group A *Streptococcus* cell-wall polysaccharide. The hexapeptide binds to the monoclonal antibody SA-3, mimicking the branched trisaccharide repeating unit, L-Rha-α-(1 → 2)-(D-GlcNAc-*β*-(1 → 3))-α-L-Rha (Rha, rhamnose; GlcNAc, *N*-acetylglucosamine). The peptide adopts a tight turn conformation with close contacts between the side chains of valine and tyrosine. Relaxation network editing experiments (QUIET-NOESY) were used to confirm the validity of the observed contacts and to evaluate the presence of spin diffusion pathways. Saturation transfer difference (STD-NMR) experiments with selective saturation of protein resonances revealed enhancements of many of the peptide resonances due to close contacts between the peptide and the protein within the antibody combining site.

Cell-surface polysaccharides of bacteria are important as virulence factors and antigens (*1*−*4*). Some polysaccharide-based vaccines have been successfully developed (*1*−*4*); however, development has been complicated by weak immunogenic effects, particularly T-independent response without memory function, and poor response in infants (*1*−*5*). These problems have been circumvented, in some cases, by conjugation to proteins (*5*) or peptides (*6*). Glycoconjugate vaccines elicit T-dependent responses and can be used directly as antigens or as priming agents for boosting with polysaccharide (*5*). Carbohydrate-mimetic peptides (*7*−*11*) are attractive as lead candidates for vaccines because of their immunogenic potential (*12*−*19*) and their greater discrimination of complementary topographies in antibody combining sites (*8*). Such peptides present the possibility of fine-tuning of an immune response against a particular epitope (e.g., to prevent autoimmune reactions), whereas such discrimination might not be possible with carbohydrate epitopes (*8*). In several studies, phage-displayed peptide libraries have been screened with monoclonal antibodies directed against carbohydrates to obtain binding peptide sequences (*7*). Often, binding affinities are similar to or greater than those of the carbohydrates, and consensus sequences for groups of crossreactive peptides have been identified (*8*). In several cases, these peptides have been used as immunogens to elicit crossreactive carbohydrate-directed responses (*12*−*19*). Peptide-carbohydrate mimicry has also been observed with enzymes (*20*, *21*) and lectins (*22*, *23*).

As yet, there is little information regarding the origin of peptide-carbohydrate mimicry. Structural mimicry, whereby a mimetic ligand makes the same contacts to a protein receptor as a carbohydrate ligand, has been observed for mimetic *proteins*, as in the case of a camel heavy-chain antibody against lysozyme (*24*), and in α-amylase-inhibitor complexes (*25*, *26*), but not yet for mimetic peptides. The crystal structure of a peptide mimetic of *Cryptococcus neoformans* capsular polysaccharide, in complex with an antibody, has been reported, in which the peptide adopts a conformation consisting of two tight turns (*27*). However, the corresponding carbohydrate-bound structure is not available, precluding comment on the nature of mimicry. We have recently communicated our results with a monoclonal antibody directed against the *Shigella flexneri* Y *O*-antigen (*28*). Here, crystal structures of the Ab-octapeptide mimetic and Ab-pentasaccharide complexes were compared. The results indicate that although both ligands engage some common groups on the Ab receptor in hydrogen bonding and hydrophobic interactions, each ligand also displays unique interactions with the protein, lending support to our previous hypothesis that "functional" mimicry and not "structural" mimicry might be active in peptide mimicry of carbohydrates (*8*).

We have previously reported the Ab-bound conformation of a trisaccharide corresponding to the cell-wall polysaccharide (CWPS)[1] of group A *Streptococcus* by TRNOE NMR spectroscopy (*29*). Group A *Streptococcus* are pathogenic species that cause rheumatic fever, necrotizing fasciitis, and streptococcal toxic shock syndrome (*30*−*34*). Antibodies directed against the CWPS are restricted in sequence and in gene usage (*8*) and recognize, as a minimal unit, a trisaccharide representing the branch point, L-Rha-α-(1 → 2)−

[†] We are grateful to the Natural Sciences and Engineering Research Council of Canada for financial support (38227-00). We thank the Canadian National High Field NMR Centre (NANUC) for their assistance and use of the facilities. Operation of NANUC is funded by the Canadian Institutes of Health Research, the Natural Sciences and Engineering Research Council of Canada and the University of Alberta.

[‡] This work is dedicated, with respect, to the memory of Professor R. U. Lemieux, an inspiring mentor.

* To whom correspondence may be addressed. Telephone: (604) 291−4884; Fax: (604) 291−5424; E-mail: bpinto@sfu.ca.

10.1021/bi011927u CCC: $22.00
Published on Web 01/24/2002

(D-GlcNAc-β-(1 → 3))-α-L-Rha (*35*). We have used the NMR-derived trisaccharide conformation, together with comparative modeling of the Fv region of the Ab Strep 9, to derive a model for the Ab-CWPS complex (*36*). We now report the bound conformation of a peptide mimetic of CWPS, DRPVPY, to a related MAb, SA-3, by trNOE NMR spectroscopy. This IgM MAb is directed against the same carbohydrate epitope and has high homology to Strep 9 in the V_L and V_H regions (*8*). The mimetic peptide for MAb SA-3, DRPVPY, was selected from a phage-displayed library (*8*). The success of the trNOE experiment is critically dependent on the dissociation rate constants of bound ligands, and thus far, we have had success only for the MAb SA-3 system.

We emphasize that the database of such protein−ligand/protein−surrogate ligand pairs is still extremely small and that conclusions about the nature and origin of mimicry must await further structural investigations. This study serves as a prelude to the detailed comparison of the ligand topographies for a carbohydrate and its mimetic, and the nature of the Ab-ligand interactions in these complexes. To date, we have not obtained crystals of the Fab-ligand complexes (*36*).

MATERIALS AND METHODS

Reagents. The hexapeptide, DRPVPY, was synthesized and purified by HPLC at the Alberta Peptide Institute (Edmonton, Alberta). The monoclonal antibody SA-3 was purified from murine ascites fluid by precipitation with 45% saturated ammonium sulfate, followed by size-exclusion chromatography on Sephacryl HR-300 (Pharmacia) and concentration with Centriprep-30 (Millipore).

NMR Experiments. NMR samples were prepared in phosphate-buffered saline solution, pH 6.15 (12 mM phosphate, 137 mM NaCl, 3 mM KCl, 10% D_2O, 0.02% NaN_3). Preliminary experiments were performed on a Bruker AMX600 spectrometer. For measurement of the affinity constant, 1D spectra were recorded at peptide: binding site ratios of 3:1, 6:1, 10:1, 20:1, and 25:1. 2D trNOESY spectra were recorded to determine the most favorable ratio for transferred NOE effects, which was found to be 20:1. Therefore, the final sample was prepared with 3.7 mg of antibody (6.3 μM antibody; 38 nmol binding sites) and 0.57 mg of peptide (1.27 mM; 760 nmol; 20:1 peptide/binding site ratio) in 600 μL of buffer. Control samples were prepared with 0.60 mg of peptide and 3.5 mg of BSA in 600 μL of buffer. After optimization of the peptide/antibody ratio, final experiments were performed on a Varian 800 MHz spectrometer (NANUC, Edmonton, Alberta) for highest sensitivity and spectral dispersion. Resonances of the peptide were assigned based on 2D TOCSY and DQF−COSY experiments. Water suppression was achieved by presaturation or WATERGATE (*37*). Chemical shifts were referred to external DSS. 1D spectra were acquired with 48K data points. NOESY and trNOESY experiments were acquired at 298 K in phase-sensitive mode using the States (hypercomplex) method, with 8K points and 752 t_1 increments, and a relaxation delay of 1.5 s. Mixing times of 50−300 ms were used to obtain full buildup curves. QUIET-NOESY experiments (*38*, *39*) were acquired with 4K points and 640 t_1 increments, a relaxation delay of 1.5 s, and a mixing time of 200 ms. Gaussian G3 cascade pulses (6.2−6.3 ms, γB_1 = 1.0 to 1.1 kHz) applied halfway through the mixing time provided doubly selective inversion of 0.75 ppm wide bands at chosen positions in the spectrum. STD-NMR spectra (*40*−*42*) were acquired at 600 and 800 MHz. Experiments at 800 MHz were performed with selective saturation of protein resonances at 10 ppm (35 ppm for reference spectra) using a series of 40 SEDUCE pulses (50 ms, 1 ms delay between pulses, γB_1 = 0.1 kHz, excitation width approximately 100 Hz) for a total saturation time of 2 s. Subtraction of saturated spectra from reference spectra was performed by phase cycling (*40*−*42*); 8K scans were acquired for sensitivity in the difference experiment.

NMR Data Processing. Data acquired at NANUC were converted to Bruker format by XWIN-NMR (Bruker) and all further processing was performed within XWIN-NMR. The 2D NOESY data (8K × 752) were subjected to linear prediction to 852 points in F_1, followed by zero-filling to 2K points and multiplication by a squared cosine function, to give a final data matrix of 8K × 2K. The 2D QUIET-NOESY data (4K × 640) were subjected to linear prediction to 740 points in F1, followed by zero-filling to 2K points and multiplication by a squared cosine function, to give a final data matrix of 4K × 2K. 2D Fourier transformation gave the final spectra. All 2D spectra were baseline-corrected automatically prior to integration of cross-peak volumes.

Distance Information from trNOESY Spectra. Cross-peaks in 2D trNOESY spectra were integrated using XWIN-NMR. Apparent distances were calculated using the distance extrapolation method, which partially corrects for spin diffusion (*43*). Distances were not normalized to the diagonal peak intensity, as in many cases the diagonal peaks could not be resolved. The distance between the aromatic δ and ϵ protons of tyrosine (2.47 Å) was used as a reference for calibration. TrNOE buildup curves were plotted within Excel (Microsoft); apparent distances were plotted against mixing time and extrapolated to zero mixing time using a second-order polynomial.

Molecular Modeling. Distance restraints obtained from trNOESY spectra were incorporated into a simulated annealing protocol within the program XPLOR (*44*), using the parallhdg force field. Only unambiguously assigned cross-peaks were used to calculate distances, resulting in 61 distance restraints. Distance restraints to unresolved or nonstereospecifically assigned diastereotopic protons were incorporated using r^{-6} summation (*44*). Minimized structures of the peptide in either all-α_R, all-β or all-α_L conformation were used as starting points for molecular dynamics. Simulations consisted of 90 ps of molecular dynamics at 1000 K,

[1] Abbreviations: NMR, nuclear magnetic resonance; 1D and 2D, one-dimensional and two-dimensional; NOE, nuclear Overhauser effect; trNOE, transferred nuclear Overhauser effect; NOESY and trNOESY, nuclear Overhauser effect spectroscopy and transferred nuclear Overhauser effect spectroscopy; QUIET-NOESY, quenching undesirable indirect external trouble in NOESY; ROESY, rotating-frame Overhauser effect spectroscopy; TOCSY, total correlation spectroscopy; DQF−COSY, double-quantum-filtered correlation spectroscopy; WATERGATE, water suppression by gradient-tailored excitation; DSS, 3-(trimethylsilyl)-1-propanesulfonic acid; F_1 and F_2, first and second frequency dimensions; STD-NMR, saturation transfer difference NMR; Rha, rhamnose; GlcNAc, *N*-acetylglucosamine; Ab, antibody; MAb, monoclonal antibody; CWPS, cell-wall polysaccharide; Fv, variable fragment; FAb, fragment with antigen binding; V_L, variable light chain; V_H, variable heavy chain; HPLC, high-performance liquid chromatography; BSA, bovine serum albumin; rmsd, root-mean-square difference; SFU, Simon Fraser University; NANUC, National High-Field Nuclear Magnetic Resonance Centre.

Table 1: Chemical Shifts of the DRPVPY Peptide

resonance	δ (310) (ppm)[a]	δ_{lit} (298) (ppm)[b]	δ_{lit} (298) − δ (310) (ppm)
Asp-1			
Hα	4.31	4.64	
Hβ	2.90	2.72	
	2.77	2.65	
Arg-2			
HN	8.60	8.20	−0.40
Hα	4.69	4.65	−0.04
Hβ	1.88, 1.77	1.81	
Hγ	1.68	1.67	
Hδ	3.21	3.21	
HNϵ	7.14	8.07	
HNζ	6.62		
Pro-3			
Hα	4.48	4.42	−0.06
Hβ	2.28, 1.90	2.29, 1.94	
Hγ	2.04	2.02	
Hδ	3.82, 3.67	3.63	
Val-4			
HN	7.99	8.02	0.03
Hα	4.42	4.44	0.02
Hβ	2.02	2.06	
Hγ	0.93, 0.90	0.97, 0.92	
Pro-5			
Hα	4.41	4.42	0.01
Hβ	2.18, 1.93	2.29, 1.94	
Hγ	1.98	2.02	
Hδ	3.79, 3.64	3.63	
Tyr-6			
HN	7.60	8.12	0.52
Hα	4.52	4.55	0.03
Hβ	3.07, 3.01	3.03, 2.98	
Hδ	7.14	7.14	
Hϵ	6.85	6.84	

[a] Chemical shifts are reported for 10.8 mM DRPVPY in phosphate-buffered saline solution, pH 6.15 (12 mM phosphate, 137 mM NaCl, 3 mM KCl, 10% D_2O, 0.02% NaN_3) at 310 K and are relative to external DSS. [b] Chemical shift values for amino acid proton resonances in unstructured (random coil) peptides are taken from ref *46* and were measured at 298 K and pH 5.0 relative to internal DSS. For the residues followed by a proline (Arg-2, Val-4), the literature values are those reported by the authors for residues followed by proline in an unstructured peptide.

with increasing force constants for geometry and a force constant for NOE-derived distances of 50 kcal/mol·Å^2, followed by cooling to 100 K for 20 ps. The resulting structures were refined by another cooling cycle from 1000 to 100 K over 45 ps using either the CHARMm force field ($\epsilon = 4$) or the parallhdg force field, followed by 1200−1500 cycles of energy minimization using the parallhdg force field. The criteria for acceptance of structures were correct geometry and no NOE restraint violations of > 0.5 Å. Analysis of the structures was performed within InsightII (Accelrys Inc.) or MOLMOL (*45*).

RESULTS AND DISCUSSION

NMR Parameters of the Free Peptide. The NMR parameters of the free peptide revealed little evidence for organized 3D structure. Chemical shifts and J(HN−Hα) values were close to random-coil (average) values (Table 1) (*46*). The HN resonance of Arg-2 had a reduced temperature coefficient (Table 2); this usually indicates participation in an intramolecular hydrogen bond. However, in the presence of BSA or antibody, this amide proton also had a much faster exchange rate, as deduced from its low intensity and increased line width. This could possibly result from interaction with the neighboring, charged Asp residue. The cause of the slight downfield shift of this resonance is unknown; such a shift usually indicates β structure, but there is no accompanying shift of Hα, also an indicator of β structure.

Table 2: Temperature Coefficients of Amide Proton Resonances in the DRPVPY Peptide

amide proton resonance	temperature coefficient ppb/K[a]	+SA-3[b]	+BSA[c]
Arg-2	−5.8	−5.7	n.d.
Val-4	−11.4	−11.6	−10.9
Tyr-6	−13.5	−10.0	−8.2

[a] Temperature coefficients were measured in 1D ^{1}H NMR spectra recorded at 281, 285, 298, and 310 K. [b] Temperature coefficients were measured from 1D ^{1}H NMR spectra recorded at 281, 288, and 300 K. [c] Temperature coefficients were measured from 1D ^{1}H NMR spectra recorded at 298, 300, and 310 K.

Resonances attributable to minor isomers of the peptide were assigned to cis isomers about the peptide bonds to proline. The observation of chemical exchange cross-peaks in the NOESY spectrum between resonances of the major (trans) and minor (cis) isomers confirmed this assignment. The concentration of the most populated cis isomer was 20% of that of the major trans isomer.

NMR Experiments on Peptide with Antibody. In the presence of the antibody, selective line-broadening of the resonances of only the major trans isomer was observed, indicating binding of the peptide to the antibody. The affinity constant was estimated from the line-broadening at different peptide/antibody ratios (*47*) to be 5×10^4 M^{-1}. The affinity constant for the antibody binding to a hexasaccharide ligand representative of the group A *Streptococcus* CWPS was determined by microcalorimetry to be 5.71×10^4 M^{-1}, while that for the longer peptide ADGA**DRPVPY**GACG(Orn-biotin), was found to be 1.60×10^6 M^{-1} (*8*). Attempts to measure the affinity constant of the hexapeptide by microcalorimetry were unsuccessful, as the purified antibody was inactivated by precipitation during the runs. The longer peptide comprises the six-residue sequence selected by phage library screening as well as flanking residues derived from the sequence of the phage pIII protein. These measurements show that the hexapeptide DRPVPY is necessary and sufficient for binding, but residues from the phage protein do contribute additional binding energy. Specificity for the antibody is provided by the hexapeptide DRPVPY, as shown previously (*8*).

The bound conformation of the peptide was investigated by trNOESY experiments. A large number of transferred NOE contacts were observed in the presence of the antibody. These included cross-peaks indicative of contacts between Val-4 and the backbone and side chains of Arg-2, Pro-3, Pro-5, and Tyr-6; between Arg-2 and Pro-3; and between Pro-5 and Tyr-6 (Figure 1).

The increased solution viscosity upon addition of protein slows the tumbling time of molecules in solution and could lead to the appearance of negative NOEs in the free peptide, which might be mistaken for transferred NOEs resulting from the bound conformation. Therefore, a negative control was provided by recording NOESY spectra of the peptide in the presence of BSA at the same w/v concentration as was used for the antibody sample. Virtually no NOEs were observed

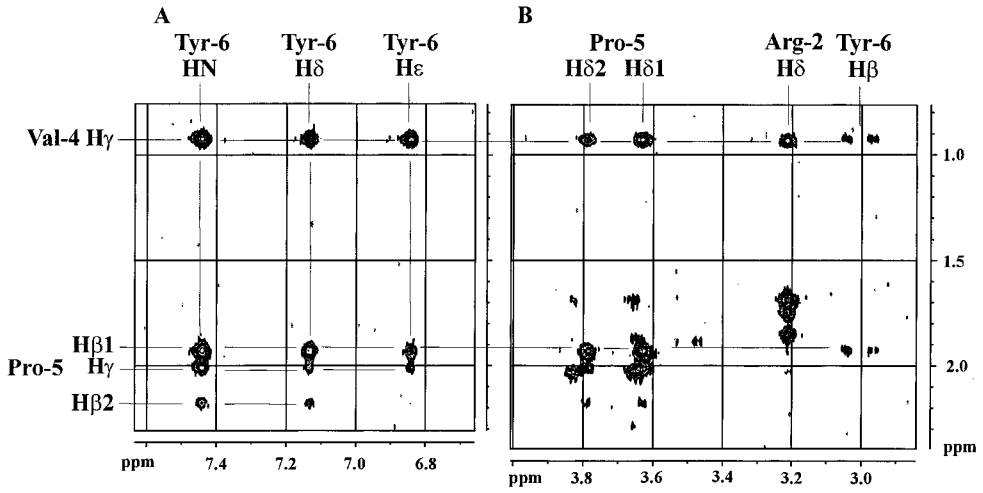

FIGURE 1: Regions of a trNOESY spectrum (τ_m = 200 ms) of the hexapeptide in the presence of the antibody, showing cross-peaks indicating contacts between the side chains of Val-4, Pro-5, and Tyr-6.

for the free peptide with BSA at 298 K. This showed that the large number of negative NOEs observed in the presence of the antibody was due to transfer from the bound peptide (transferred NOE).

Structure Calculations. The trNOESY cross-peaks were integrated and converted to distance restraints to be used in calculating the bound conformation. A lower distance bound of 1.8 Å was used for all distances, while the upper distance bound was set to the calculated distance +1.0 Å. The r^{-6} summation method (*44*) was used to calculate distances to unresolved or nonstereospecifically assigned diastereotopic protons; correspondingly, peak intensities were not corrected for multiplicity. The distance restraints were incorporated into a simulated annealing protocol within XPLOR (*44*). A set of 40 structures produced by simulated annealing were subjected to refinement and energy minimization, followed by checks for correct geometry and agreement with the distance restraints. Of 40 structures produced by simulated annealing, 27 were judged to be acceptable by these criteria. All of the latter adopted a very similar conformation, comprising a well-defined tight turn in the last three residues of the peptide, VPY (Figure 2A). This is also apparent from the contacts between the side chains of these residues in the trNOESY spectra (Figure 1). The tight turn is stabilized by association between the hydrophobic side chains of VPY, as shown by van der Waals contacts between the side chains; representative distances in the average structure (Figure 2B) are Val-4 Cγ1−Tyr-6 Cϵ1 3.98 Å, Val-4 Cγ1−Tyr-6 Cδ1 4.10 Å, and Pro-5 Cβ−Tyr-6 Cδ1 3.76 Å. The Val residue adopted an unusual conformation with a positive ϕ angle (ϕ = 89°; Table 3A), corresponding to the α_L region of the Ramachandran map. This is uncommon for any residue but glycine. The 27 structures superimposed with rmsd = 0.11 Å for backbone atoms, or 0.80 Å for all heavy atoms, considering residues Val-4 to Tyr-6 (Figure 2A). There is more disorder in the first part of the peptide, DRP, which is less well-defined by the trNOEs. The derivation of restraints in this part of the peptide was hampered by spectral overlap of the Val-4 Hβ and Pro-5 Hγ resonances, and of the Val-4, Pro-5 and Tyr-6 Hα resonances. In addition, the Arg HN resonance was so broad ($\Delta\nu_{1/2}$ estimated at 44 Hz) that no trNOE cross-peaks involving this proton were observed. Nevertheless, contacts between the Arg-2 and Val-4 side chain provided some restraints on the conformation. If the entire peptide is considered, the 27 structures superimpose with rmsd = 0.24 Å for backbone atoms or rmsd = 1.16 Å for all heavy atoms.

The calculation was repeated using restraining terms to prevent left-handed turns (positive ϕ angles). This procedure decreased the fraction of accepted structures to 10%; those that were acceptable were very similar to those obtained in the first simulations, but with a more usual β conformation (ϕ = −175°; Table 3B, Figure 2C−E) for the Val-4 residue.

Table 3: Backbone Dihedral Angles (°) in the Bound Conformation of the Hexapeptide[a]: (A) Using Only TrNOE-Derived Restraints[b] and (B) with All ϕ Dihedral Angles Restrained to Negative Values[c]

	A		B	
residue	ϕ (C′−N−Cα−C)	ψ (N−Cα−C−N′)	ϕ (C′−N−Cα−C)	ψ (N−Cα−C−N′)
Asp-1		−125		146
Arg-2	−171	143	−173	155
Pro-3	−50	139	−61	−172
Val-4	89	81	−175	80
Pro-5	−34	−27	−34	−35
Tyr-6	−140		−124	

[a] Average of all accepted calculated conformations. [b] Average of 27 structures. [c] Average of four structures.

Evaluation of Spin Diffusion. The possibility for error caused by spin diffusion in transferred NOESY experiments has been investigated by others in both theoretical and experimental studies (*38*, *39*, *48*−*55*). However, in many experimental studies, the extent of such error is not rigorously evaluated. Such evaluation is particularly important in studies with very large protein receptors, since the cross-relaxation rate in the bound state is increased (*56*). Therefore, we chose to investigate the effects of spin diffusion in detail. Some of the trNOE buildup curves showed unusual shapes due to gains or losses from spin diffusion (Figure 3). The distance extrapolation method (*43*) was used in calculating distances to bias the intensity measurements toward initial values that are less affected by spin diffusion.

The QUIET-NOESY (quenching of undesired indirect external trouble in NOESY) technique (*38*, *39*) is a method of "relaxation network editing", or selectively eliminating

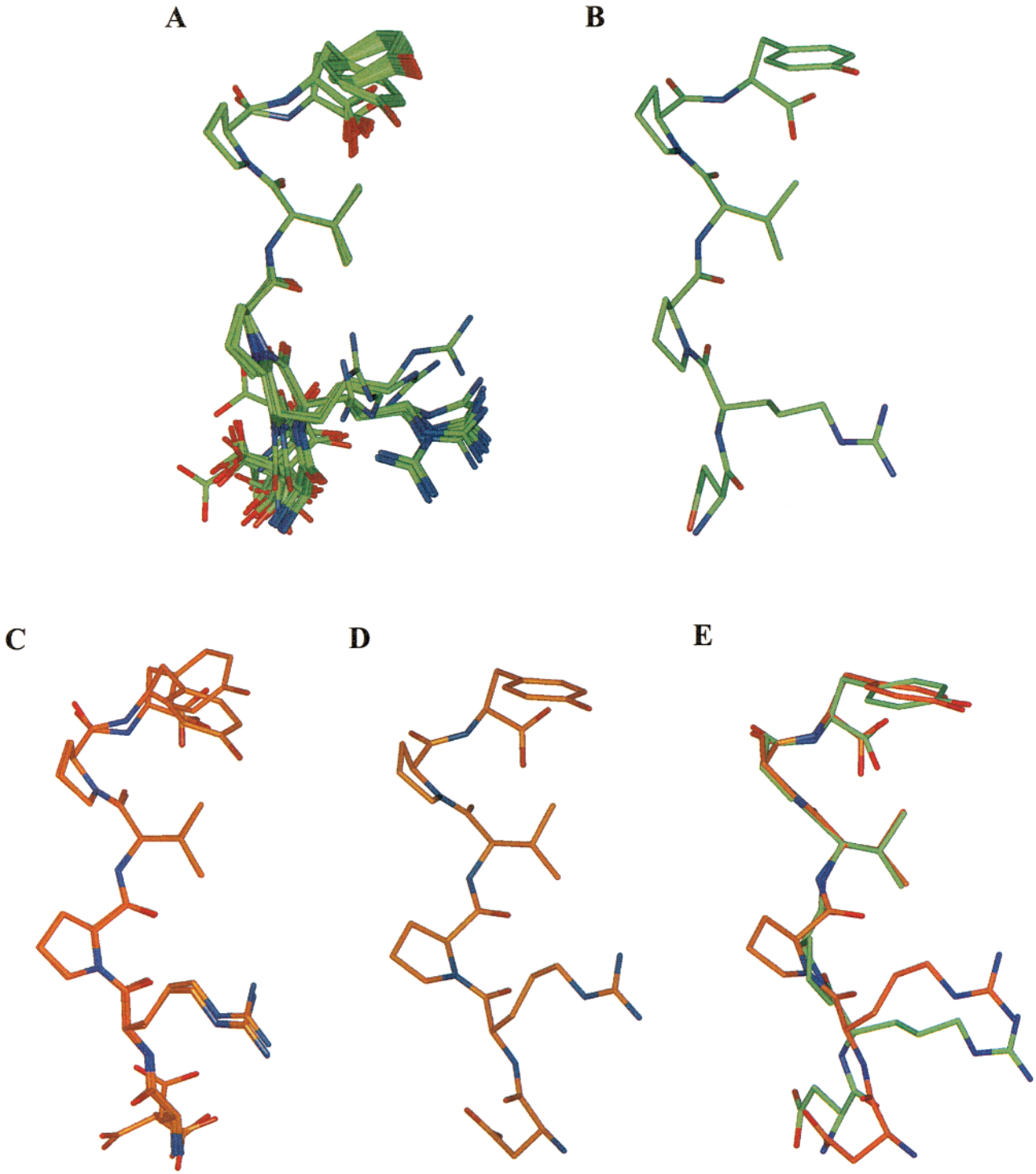

FIGURE 2: Bound conformations of the hexapeptide. Superposition of structures was performed within InsightII and is based on the backbone atoms of residues 4−6. (A) Family of 27 structures calculated using trNOE-derived restraints only. (B) Average of the 27 structures in panel A. (C) Family of four structures calculated with all ϕ dihedral angles restrained to negative values. The peptide is colored differently for purposes of comparison in panel E. (D) Average of the four structures in panel C. (E) Average structures from both calculations, showing the very similar tight turn.

indirect cross-relaxation pathways, allowing observation of direct pathways only. In this experiment, a doubly band-selective inversion pulse is inserted halfway through the NOESY mixing time, so that the buildup of NOE between inverted and noninverted spins changes sign and is canceled by the time of the observation pulse. This allows evaluation of an NOE cross-peak by placing each resonance of interest within the two inversion bands; NOE cross-peaks observed are then due only to direct cross-relaxation between the two spins, while spin diffusion contributions from resonances outside the bands are canceled to first order (*39*).

Therefore, several of the most interesting cross-peaks appearing only in the presence of antibody were chosen for evaluation by QUIET-trNOESY spectra recorded at 800 MHz. These included, for example, Arg-2 Hδ−Val-4 Hγ, indicating proximity between the Val-4 and Arg-2 side

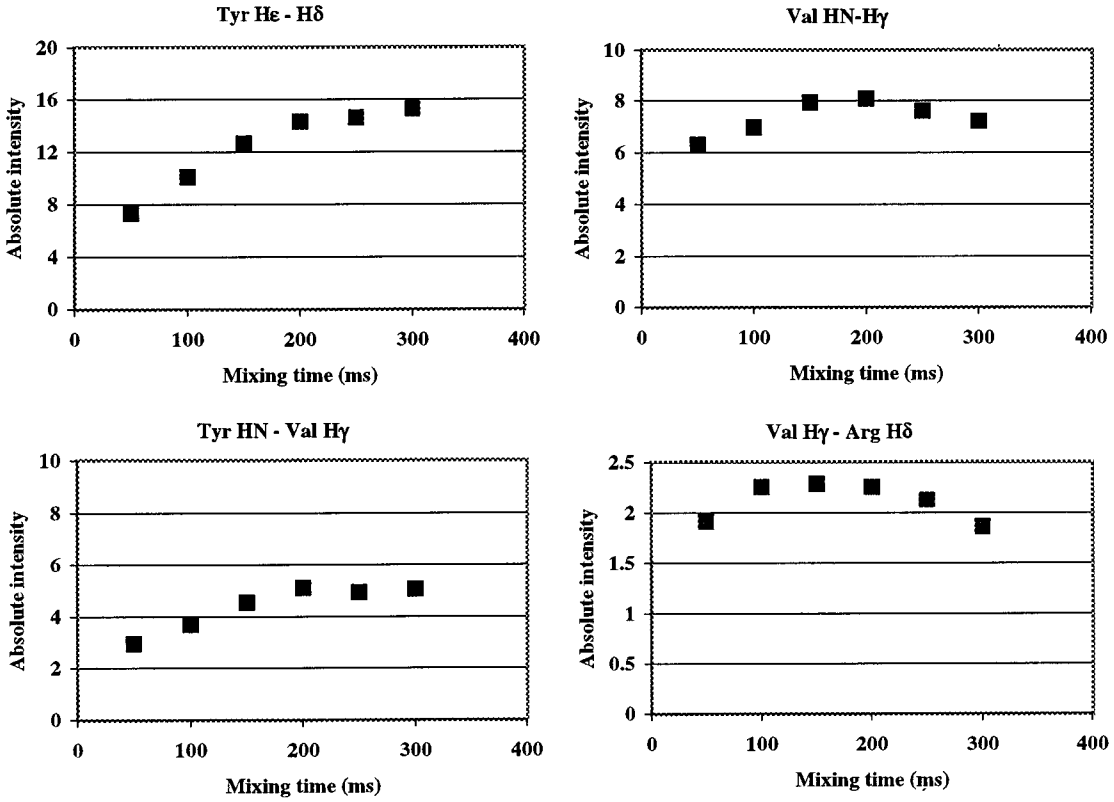

FIGURE 3: Representative trNOESY buildup curves.

chains; contacts between the Val-4 and Tyr-6 residues and the Pro-3,-5 Hδ protons, representative of the geometry of the turn; and contacts between the Pro-5 Hδ and Tyr-6 Hβ protons and Val-4 Hγ, longer-range contacts which could possibly have arisen from spin diffusion. QUIET-trNOESY spectra with a mixing time of 200 ms and with inversion of bands containing these resonances were recorded at 800 MHz. As shown in Figure 4, almost all of these contacts were still present in the QUIET-NOESY spectra, showing that they are truly representative of close contacts between protons and not due to indirect pathways. The only exception is the contact between Val HN and Pro-3 Hδ_2, which disappears in the QUIET-trNOESY spectrum (Figure 4). This contact was therefore judged to be due to spin diffusion. The first set of calculations was then repeated, with this distance restraint eliminated from the calculation. Interestingly, a nearly identical conformation resulted, showing that inclusion of this spurious contact, in the presence of many others, had not led to an incorrect result.

The bands connecting quiet windows in the QUIET-NOESY spectrum should, in theory, be empty, as all indirect pathways are canceled. However, residual contacts at ~10−25% of the intensity in NOESY were observed in the quiet bands. The individual contacts observed, and their intensities, varied depending on the position of the inversion bands. This is most likely due to second-order effects. Because the rate of NOE buildup is not necessarily the same in the first and second halves of the mixing time, some contacts may not be completely canceled. Therefore, for most purposes the shortest mixing time possible should be used. This information may, however, be used to identify possible spin diffusion pathways, which may be confirmed by other means. As shown in Figure 5, an incompletely canceled cross-peak

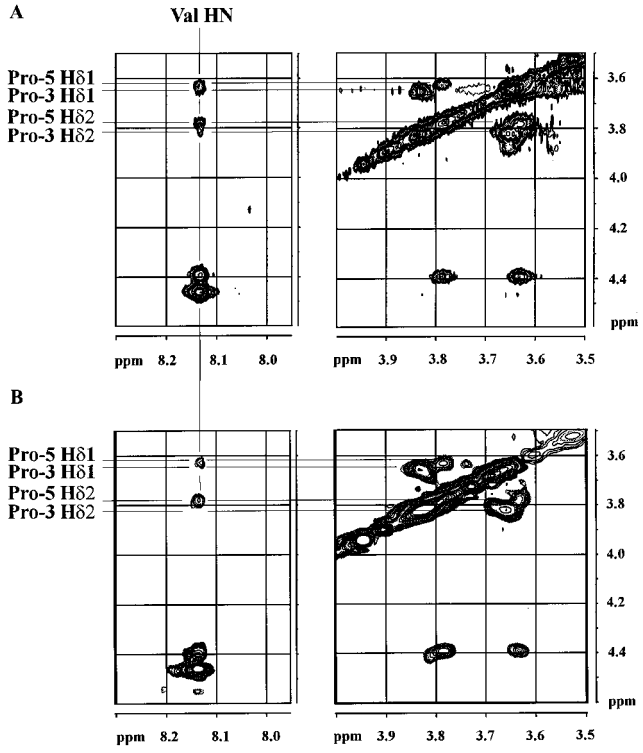

FIGURE 4: TrNOESY and QUIET-trNOESY spectra of the peptide in the presence of antibody. (A) Regions of a trNOESY spectrum (τ_m = 200 ms) showing Val-4 HN−Pro-3,-5 Hδ cross-peaks and Pro-3,-5 Hδ−Hδ cross-peaks. (B) Corresponding regions of a QUIET-trNOESY spectrum (τ_m = 200 ms) with inversion of 0.75 ppm wide bands centered at 4.15 and 8.1 ppm; within the intersection of the quiet bands (quiet window), the Val HN−Pro-5 Hδ cross-peaks are still present, while the Val HN−Pro-3 Hδ_2 cross-peak is absent, indicating cancellation due to spin diffusion.

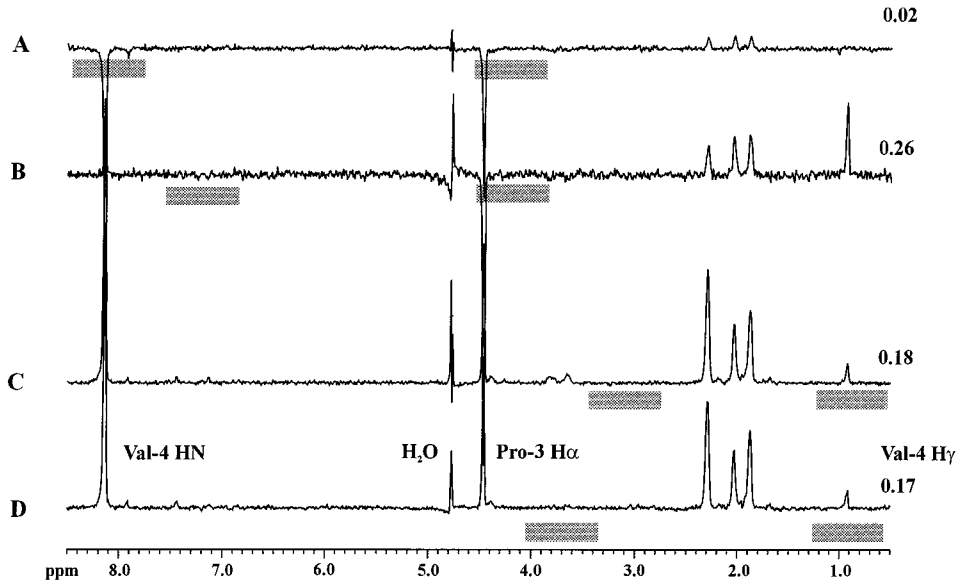

FIGURE 5: Traces from 2D QUIET-trNOESY spectra taken at 4.46 ppm in F_1, Pro-3 Hα resonance frequency. Inverted bands are indicated by shaded bars below the traces. In each trace the absolute intensity of the Val-4 Hγ resonance, relative to the Pro-3 Hα diagonal resonance in panel C, is given. This signal is present in panels B, C, and D due to incomplete cancellation (second-order effects). However, in trace A, when Val-4 HN is also inverted, the Val-4 Hγ signal becomes completely canceled, indicating a possible spin diffusion pathway from Pro-3 Hα to Val-4 HN to Val-4 Hγ.

between Pro-3 Hα and Val-4 Hγ is present in all the spectra, except that in which Val HN is also inverted. This indicates a possible spin diffusion pathway between Pro-3 Hα, Val HN, and Val Hγ. Again, the calculations were repeated with this distance restraint eliminated, and a very similar conformation resulted. Therefore, although spin diffusion may contribute to the observed intensity of the Pro-3 Hα−Val Hγ trNOE contact, inclusion of this distance restraint had not led to bias in the calculated conformation. The results from eliminating this distance restraint as well as the Val HN−Pro-3 Hδ_2 distance restraint are consistent with general findings that the observation of a large number of NOEs can lead to an accurate conformation even if the margin of error for each individual NOE is quite large (*57*). It may be noted that although the presence of second-order effects in QUIET-NOESY is generally undesirable, and should be taken as a warning to carefully evaluate the intensities of contacts in the quiet windows, these effects may also provide information that is useful in identifying spin-diffusion pathways.

Further Considerations Regarding Spin Diffusion. The QUIET-NOESY experiment cannot remove indirect pathways occurring due to spins whose resonance frequency happens to be within the bands of inversion. Therefore, the experiments described above did not exclude spin diffusion between, for example, the geminal methylene protons of the proline residues. This situation is a possibility, as certain contacts to protons on one side of the Pro-3,-5 rings are observed in the free peptide spectrum (data not shown), while contacts to the other side appear in the presence of antibody. This could be due to an increase in the intensities of trNOEs over ROEs of the free peptide or to the selection of a conformation for binding which does not predominate in solution. In addition, spin diffusion by a close ligand proton has been shown to be less important than that by a close protein proton in its effect on the trNOE buildup rate (*48*). However, the possibility still existed that these contacts were due to intraligand spin diffusion. As a test, the calculations were repeated with some of these contacts excluded. The only contact whose absence affected the conformation was that between Val-4 HN and Pro-3 Hβ_2. When this contact was excluded from the calculation, there was some variation in the ϕ angle of Val-4, with half of the structures adopting the α_L conformation as before ($\phi = 90-110°$), while the other half adopted a β conformation ($\phi = 140°$). This made little difference to the calculated structure, as the overall conformation of the rest of the peptide was maintained.

Bound Conformation. We conclude, therefore, that the peptide adopts a tight turn conformation in the bound state. The turn is well defined by the backbone torsion angles of Pro-5 and Tyr-6 and the ψ angle of Val-4. The characteristic trNOEs were shown to be valid by QUIET-trNOESY experiments. Some of the remaining contacts may have some contributions from spin diffusion, causing some uncertainty in the ϕ angle of Val-4. However, this does not affect the overall conformation of the molecule significantly. The DRP portion of the peptide is also in a turn conformation, which is less well-defined by the available trNOEs. Nevertheless, we show that the conformation includes contacts between the Arg-2 and Val-4 side chains.

Turn Conformations in VPY Segments. TrNOE contacts between the Tyr-6 HN, Hδ and Hϵ protons and the Val-4 Hγ protons were also observed in preliminary experiments with the antibody and a longer peptide, ADGA**DRPVPY**G-ACG(Orn-biotin), representing the six-residue sequence selected by phage library screening within the context of the phage pIII protein. These contacts suggest the presence of a similar bound conformation with a tight turn centered on Pro-5. These contacts as well as a contact between Pro-5 Hδ_1 and Val-4 Hγ were also observed in the ROESY spectrum of the hexapeptide DRPVPY in the absence of antibody. This observation suggests that turn conformations with hydrophobic association between the VPY side chains are also populated to a certain extent in solution. This

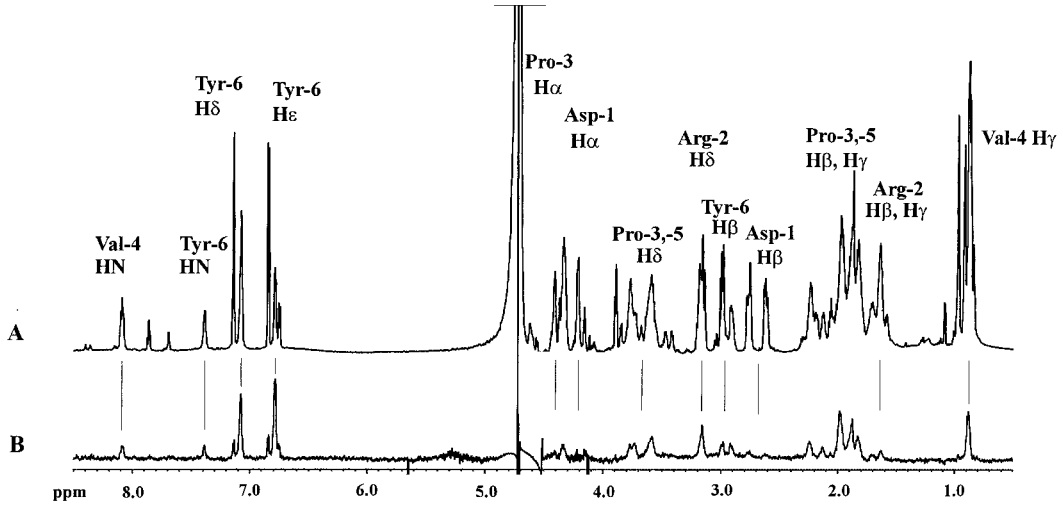

FIGURE 6: (A) 1D ^{1}H NMR spectrum of the peptide in the presence of the antibody. (B) STD-NMR spectrum of the peptide in the presence of the antibody, showing enhancements of resonances of protons making close contacts with the antibody combining site.

conclusion is in agreement with other studies showing that turn conformations may be populated in several short peptides, representing antigenic regions of proteins, in solution (*58, 59*).

Mode of Peptide Binding. The well-defined VPY segment of the peptide does not completely comprise the consensus sequence found from phage-displayed library screening; rather, RPXXY was the consensus sequence isolated (*8*). In particular, the RP residues were shown to be critical for binding and could not be substituted (*8*).

After prolonged storage of the samples, hydrolysis of the peptide, presumably by residual proteases present in the antibody preparation, was noted. The hydrolytic reaction was a specific cleavage of the Tyr-6 residue, as shown by electrospray mass spectrometry. Interestingly, the cleaved fragment did not give rise to transferred NOEs, as shown by recording a trNOESY spectrum of a sample containing completely hydrolyzed peptide; therefore, the Tyr-6 residue is required for binding.

To provide additional information regarding the peptide's mode of binding, saturation transfer difference (STD-NMR) experiments were performed. The STD-NMR technique (*40*−*42*) is a method of epitope mapping by NMR spectroscopy. Resonances of the protein are selectively saturated over a period of time, allowing NOE enhancements to develop over many resonances of the protein, and in addition, giving rise to intermolecular NOE effects with a binding ligand. If the 1D ^{1}H NMR spectrum of the ligand is then recorded and subtracted from a 1D spectrum recorded without saturation of the protein, these intermolecular negative NOE effects are observed as enhancements of the signals of protons that are in close contact with the protein. This allows determination of the binding epitope, or the areas of the ligand actually contacting the binding site.

The STD-NMR spectrum of the hexapeptide in the presence of the antibody is shown in Figure 6. Almost all resonances of the peptide are enhanced, with the exception of the Asp-1 Hα and Hβ resonances, showing that all but the first residue of the peptide are in contact with the binding site. The Pro-3 Hα and Arg Hβ/Hγ resonances also show smaller enhancements. However, parts of the Arg-2 side chain are clearly involved in binding, as the Arg-2 Hδ protons are significantly enhanced. It may also be noted that the more populated (20%) cis isomer of the peptide does not bind significantly.

Turn conformations are commonly observed in antibody-peptide crystal structures (*60*), and the turn is often important in allowing peptide side chains to be positioned correctly within the binding site and to make specific contacts with residues within the site. This is clearly important here, as is shown by the epitope mapping data where all side chains except Asp-1 contact the site.

Such information is valuable in the understanding of peptide-carbohydrate mimicry and in the design of peptidomimetics, where knowledge of the specific residues required for binding is necessary.

Summary. The data presented here show that binding of the carbohydrate-mimetic peptide, DRPVPY, by the antibody SA-3 occurs with the peptide in a tight turn conformation stabilized by hydrophobic association between the VPY side chains. Specific contacts to the antibody are made by all amino acid side chains except that of Asp-1. Knowledge of the bound conformation and mode of interaction of the peptide with the antibody will be used as a starting point for further investigations of this system, with the goal of elucidating the basis of peptide-carbohydrate mimicry. Thus, NMR experiments as described above, in combination with molecular modeling, will aid in the design of new peptides, glycopeptides, and peptidomimetics with potentially greater binding affinity.

ACKNOWLEDGMENT

We are grateful to Dr. Stéphane Gagné and Dr. Ryan McKay for recording the 800 MHz NMR spectra and to Dr. Moriz Mayer for STD-NMR pulse programs. We thank Dr. Ryan McKay and Dr. Leo Spyracopoulos for their expert work in developing the Varian versions of the STD-NMR pulse programs. In addition, we thank Drs. Alan S. Tracey, Brian D. Sykes, Thomas Weimar, and Sébastien J. F. Vincent for helpful discussions.

REFERENCES

1. Jennings, H. J. (1990) *Curr. Top. Microbiol. Immunol. C 125*, 373−389.

2. Jennings, H. J. (1988) *Adv. Exp. Med. Biol. 228*, 495−550.
3. Lee, C.-J. (1987) *Mol. Immunol. 24*, 1005−1019.
4. Jennings, H. J. (1983) *Adv. Carbohydr. Chem. Biochem. 41*, 155−208.
5. Lindberg, A. A. (1999) *Vaccine 17 Suppl. 2*, S28−S36.
6. Alexander, J., del Guercio, M.-F., Maewal, A., Qiao, L., Fikes, J., Chesnut, R. W., Paulson, J., Bundle, D. R., DeFrees, S., and Sette, A. (2000) *J. Immunol. 164*, 1625−1633.
7. Zwick, M. B., Shen, J., and Scott, J. K. (1998) *Curr. Opin. Biotechnol. 9*, 427−438.
8. Harris, S. L., Craig, L., Mehroke, J. S., Rashed, M., Zwick, M. B., Kenar, K., Toone, E. J., Greenspan, N., Auzanneau, F.-I., Marino-Albernas, J.-R., Pinto, B. M., and Scott, J. K. (1997) *Proc. Natl. Acad. Sci. U.S.A. 94*, 2434−2439.
9. Valadon, P., Nussbaum, G., Boyd, L. F., Margulies, D. H., and Scharff, M. D. (1996) *J. Mol. Biol. 261*, 11−22.
10. Pinilla, C., Appel, J. R., Campbell, G. D., Buencamino, J., Benkirane, N., Muller, S., and Greenspan, N. S. (1998) *J. Mol. Biol. 283*, 1013−1025.
11. Moe, G. R., Tan, S., and Granoff, D. M. (1999) *FEMS Immunol. Med. Microbiol. 26*, 209−226.
12. Westerink, M. A. J., Giardina, P. C., Apicella, M. A., and Kieber-Emmons, T. (1995) *Proc. Natl. Acad. Sci. U.S.A. 92*, 4021−4025.
13. Agadjanyan, M., Luo, P., Westerink, M. A. J., Carey, L. A., Hutchins, W., Steplewski, Z., Weiner, D. B., and Kieber-Emmons, T. (1997) *Nature Biotechnology 15*, 547−551.
14. Phalipon, A., Folgori, A., Arondel, J., Sgaramella, G., Fortugno, P., Cortese, R., Sansonetti, P. J., and Felici, F. (1997) *Eur. J. Immunol. 27*, 2620−2625.
15. Luo, P., Agadjanyan, M., Qiu, J., Westerink, M. A. J., Steplewski, Z., Kieber-Emmons, T. (1998) *Mol. Immunol. 35*, 865−879.
16. Pincus, S. H., Smith, M. J., Jennings, H. J., Burritt, J. B., and Glee, P. M. (1998) *J. Immunol. 160*, 293−298.
17. Hutchins, W. A., Kieber-Emmons, T., Carlone, G. M., and Westerink, M. A. (1999) *Hybridoma 18*, 121−128.
18. Luo, P., Canziani, G., Cunto-Amesty, G., and Kieber-Emmons, T. (2000) *J. Biol. Chem. 275*, 16146−16154.
19. Grothaus, M. C., Srivastava, N., Smithson, S. L., Kieber-Emmons, T., Williams, D. B., Carlone, G. M., and Westerink, M. A. (2000) *Vaccine 18*, 1253−1263.
20. Eichler, J., Lucka, A. W., Pinilla, C., and Houghten, R. A. (1995) *Mol. Diversity 1*, 233−240.
21. Pan, O. C.-C. (1999) M. Sc. Thesis, Simon Fraser University, Burnaby, B. C., Canada.
22. Ravindranath, R. M. H., Tam, W.-Y., Nguyen, P., and Fincham, A. G. (2000) *J. Biol. Chem. 275*, 39654−39661.
23. Cunto-Amesty, G., Dam, T. K., Luo, P., Monzavi-Karbassi, B., Brewer, C. F., Van Cott, T. C., and Kieber-Emmons, T. (2001) *J. Biol. Chem. 276*, 30490−30498.
24. Transue, T. R., De Genst, E., Arbabi Ghahroudi, M., Wyns, L., and Muyldermans, S. (1998) *Proteins Struct. Funct. Genet. 32*, 515−522.
25. Machius, M., Vértésy, L., Huber, R., and Wiegand, G. (1996) *J. Mol. Biol. 260*, 409−421.
26. Bompard-Gilles, C., Rousseau, P., Rougé, P., and Payan, F. (1996) *Structure 4*, 1441−1452.
27. Young, A. C. M., Valadon, P., Casadevall, A., Scharff, M. D., and Sacchettini, J. C. (1997) *J. Mol. Biol. 274*, 622−634.
28. Pinto, B. M., Scott, J. K., Harris, S. L., Johnson, M. A., Bundle, D. R., Chervenak, M. C., Vyas, M. N., Vyas, N. K., and Quiocho, F. A. (1998) XIX International Carbohydrate Symposium, San Diego, U.S.A., Abstr. CP 132, CO 019.
29. Weimar, T., Harris, S. L., Pitner, J. B., Bock, K., and Pinto, B. M. (1995) *Biochemistry 34*, 13672−13681.
30. Read, S. E., and Zabriskie, J. B. (Eds.) (1980) *Streptococcal Diseases and the Immune Response*, Academic Press, New York.
31. Bisno, A. L. (1985) in *Principles and Practice of Infectious Diseases*, 2nd Ed. (Mandell, G. L., Douglas, R. G., and Bennett, J. E., Eds.), p 1133, Wiley, New York.
32. Nowak, R. (1994) *Science 264*, 1665.
33. Stevens, D. L. (1997) *Immunol. Invest. 26*, 129−150.
34. Weiss, K. A., Laverdiere, M. (1997) *Can. J. Surg. 40*, 18−25.
35. Reimer, K. B., Gidney, M. A. J., Bundle, D. R., and Pinto, B. M. (1992) *Carbohydr. Res. 232*, 131−142.
36. Pitner, J. B., Beyer, W. F., Venetta, T. M., Nycz, C., Mitchell, M. J., Harris, S. L., Mariño-Albernas, J. R., Auzanneau, F.-I., Forooghian, F., and Pinto, B. M. (2000) *Carbohydr. Res. 324*, 17−29.
37. Piotto, M., Saudek, V., and Sklenar, V. (1992) *J. Biomol. NMR 2*, 661−666.
38. Zwahlen, C., Vincent, S. J. F., Di Bari, L., Levitt, M. H., and Bodenhausen, G. (1994) *J. Am. Chem. Soc. 116*, 362−368.
39. Vincent, S. J. F., Zwahlen, C., and Bodenhausen, G. (1996) *J. Biomol. NMR 7*, 169−172.
40. Mayer, M., and Meyer, B. (1999) *Angew. Chem., Int. Ed. Engl. 38*, 1784−1788.
41. Klein, J., Meinecke, R., Mayer, M., and Meyer, B. (1999) *J. Am. Chem. Soc. 121*, 5336−5337.
42. Mayer, M., and Meyer, B. (2001) *J. Am. Chem. Soc. 123*, 6108−6117.
43. Baleja, J. D., Moult, J., and Sykes, B. D. (1990) *J. Magn. Reson. 87*, 375−384.
44. Brünger, A. T. (1992) *XPLOR (Version 3.1): A System for X-ray Crystallography and NMR*, Yale University Press, New Haven.
45. Koradi, R., Billeter, M., and Wüthrich, K. (1996) *J. Mol. Graphics 14*, 51−55.
46. Wishart, D. S., Bigam, C. G., Holm, A., Hodges, R. S., and Sykes, B. D. (1995) *J. Biomol. NMR 5*, 67−81.
47. Dwek, R. A. (1973) *Nuclear Magnetic Resonance (N. M. R.) in Biochemistry: Applications to Enzyme Systems*, Clarendon Press, Oxford.
48. Zheng, J., and Post, C. B. (1993) *J. Magn. Reson. B 101*, 262−270.
49. Lippens, G. M., Cerf, C., and Hallenga, K. (1992) *J. Magn. Reson. 99*, 268−281.
50. Campbell, A. P., and Sykes, B. D. (1993) *Annu. Rev. Biophys. Biomol. Struct. 22*, 99−122.
51. Lian, L. Y., Barsukov, I. L., Sutcliffe, M. J., Sze, K. H., and Roberts, G. C. K. (1994) *Methods Enzymol. 239*, 657−700.
52. Moseley, H. N. B., Curto, E. V., and Krishna, N. R. (1995) *J. Magn. Reson. B 108*, 243−261.
53. Arepalli, S. R., Glaudemans, C. P. J., Daves, G. D., Jr., Kovac, P., and Bax, A. (1995) *J. Magn. Reson. B 106*, 195−198.
54. Vincent, S. J. F., Zwahlen, C., Post, C. B., Burgner, J. W., and Bodenhausen, G. (1997) *Proc. Natl. Acad. Sci. U.S.A.* 94, 4383−4388.
55. Haselhorst, T., Espinosa, J.-F., Jiménez-Barbero, J., Sokolowski, T., Kosma, P., Brade, H., Brade, L., and Peters, T. (1999) *Biochemistry 39*, 12778−12788.
56. Kalk, A., and Berendsen, H. J. C. (1976) *J. Magn. Res. 24*, 343−366.
57. Neuhaus, D., and Williamson, M. P. (2000) *The Nuclear Overhauser Effect in Structural and Conformational Analysis*, 2nd ed. Wiley-VCH, New York.
58. Dyson, H. J., Rance, M., Houghten, R. A., Lerner, R. A., and Wright, P. E. (1988) *J. Mol. Biol. 201*, 161−200.
59. Campbell, A. P., Wong, W. Y., Irvin, R. T., and Sykes, B. D. (2000) *Biochemistry 39*, 14847−14864.
60. Stanfield, R. L., and Wilson, I. A. (1995) *Curr. Opin. Struct. Biol. 5*, 103−113.

BI011927U